

### Coupled Electron-Hole Transport

U. Sivan,<sup>(a)</sup> P. M. Solomon, and H. Shtrikman<sup>(b)</sup>

IBM Research, T. J. Watson Research Center, P.O. Box 218, Yorktown Heights, New York 10598

(Received 7 August 1991)

We report on transport measurements in a novel system composed of two parallel 2D electron and hole gases separated by a barrier which is high enough to prevent tunneling and recombination while thin enough to allow for strong interlayer Coulomb interaction. Separate electrical contacts to each layer and independent control of both carrier densities facilitate a detailed study of the electron-hole interaction. Current driven in one layer is found to induce opposite current in the other layer. The measured electron-hole momentum-transfer rate is a factor of 5 to an order of magnitude larger than in previous experiments on electron-electron scattering and calculations based on Coulomb scattering theory.

PACS numbers: 73.50.Dn

Sixteen years ago, Shevchenko [1], and Lozovik and Yudson [2], proposed a new electronic system composed of two parallel 2D electron (2DEG) and hole (2DHG) gases separated by a barrier which is high enough to prevent tunneling and recombination while thin enough to allow for strong Coulomb interaction between carriers on opposite sides of the barrier. In a series of theoretical papers they argued that at low temperatures, electrons and holes (*e* and *h*) should pair together to form oriented excitons which may condense and display a superfluid ground state and possibly a new type of superconductivity where phonon-mediated attraction is replaced by a Coulomb one. Although the possibility of exciton condensation in such structures is still controversial, these pioneering papers have inspired a considerable body of theoretical work on various thermodynamic and transport aspects of such a system including the effects of strong magnetic fields [3-6] and coupled charge excitations [7]. Those studies reveal a complex system with a variety of possible phases. Despite the potential interest, we are aware of only a few experiments (e.g., Refs. [8,9]) aimed to probe these ideas, all of them employing optical excitation and probing.

In this Letter we present the first transport measurements in such a system where we find interlayer momentum transfer rates which are a factor of 5 to an order of magnitude larger than theoretical predictions and related measurements in electron-electron (*e-e*) systems [10,11]. Unlike previous *e-h* experiments, in the present structure carriers are induced electrically by field effect and probed directly by magnetotransport techniques. The density of each carrier type can independently be controlled, and separate electrical contacts facilitate application of a different electric field to each of the layers (in case of *e-h* binding, a different electric field to the two constituents of an "atom").

The structure is shown in Fig. 1. It was grown by molecular-beam epitaxy on an *n*<sup>+</sup> GaAs substrate. The layers consist of (in growth order) an *n*<sup>+</sup> buffer layer, 3000-Å intrinsic GaAs, 200-Å AlGaAs barrier, 500-Å intrinsic GaAs, 2000-Å *n*<sup>-</sup> ( $1 \times 10^{16} \text{ cm}^{-3}$ ) GaAs, 1000-Å *n* ( $1 \times 10^{17} \text{ cm}^{-3}$ ) GaAs, and 2000-Å *n*<sup>+</sup> cap layer. Upon biasing the cap layer negatively with respect to the

substrate, electron and hole wells are formed on opposite sides of the AlGaAs barrier (Fig. 1). To supply holes and electrical contacts to the 2DHG, the structure is dry etched in the contact regions down to the AlGaAs barrier and beryllium implanted. The implanted region is later contacted using standard PtTi *p*-type Ohmic contacts. To prevent electronic conduction parallel to the 2DEG, the top layer is etched off everywhere except for the contacts. Electrical contact to the 2DEG is formed by standard NiGeAu alloyed contacts to the *n*<sup>+</sup> regions. Finally, a metal gate is deposited on top of the etched region. The sample is processed in a Hall bar shape of different sizes.

The electron concentration *n* and hole concentration *p* can be controlled separately by appropriate biasing of the top gate and the substrate with respect to the 2DEG and 2DHG, respectively (*V*<sub>GN</sub> and *V*<sub>SUB</sub> in Fig. 1). Extensive study of the structure reveals an independence of *n* upon *V*<sub>SUB</sub> and, conversely, *p* upon *V*<sub>GN</sub>, except for low carrier densities where screening is apparently reduced. The dependencies of *p* and *n* upon the corresponding gate voltages or bias across the barrier agree remarkably well with the expected capacitances. The barrier capacitance corresponds to an interlayer separation of 250 Å as expected from a 200-Å barrier plus the width of the wave functions

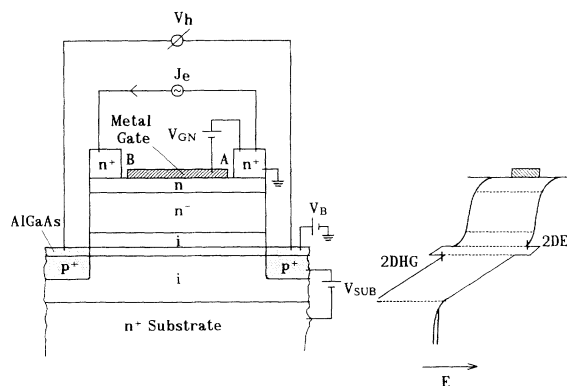


FIG. 1. The structure and schematics of the measurement circuit. On the right-hand side, the band diagram under typical bias is shown.

when confined by the strong electric field. Calculations show that under the experimental conditions, only a single electron and hole subband is populated.

The circuit used in the experiment is shown in Fig. 1. A 28-Hz ac current is applied to one layer and the induced voltage is measured across the other layer in a four-terminal configuration. The ratio between the measured voltage, corrected for the Hall bar aspect ratio, and the applied current yields the transimpedance  $R_T$ , which is a direct measure of the rate,  $\tau_{h-e}^{-1}$  ( $\tau_{e-h}^{-1}$ ), at which momentum is transferred from the 2DEG (2DHG) to the 2DHG (2DEG),  $R_T = m/e^2 p \tau_{h-e} = M/e^2 n \tau_{e-h}$  ( $m$  and  $M$  being the electron and hole effective masses, respectively). A standard measurement of intralayer resistances and low magnetic-field Hall effect provide the two carrier densities and mobilities. As expected, the induced voltage is of the same polarity as the driving voltage and opposite

compared with previous experiments on electron-electron mutual drag [10,11]. The induced voltage is linear in the applied current and the transimpedance practically satisfies the Onsager relation for all temperatures above 9 K.

The measured transimpedance versus electron density for  $p \approx 5 \times 10^{10} \text{ cm}^{-2}$  (see remark later) at three temperatures is depicted by solid symbols in Fig. 2(a). At high densities ( $\geq 5 \times 10^{10} \text{ cm}^{-2}$ ),  $R_T \propto n^{-a}$  with  $a$  varying between 2.2 at the lower temperatures and 2 at the higher ones. As the electron density is reduced, the transimpedance seems to saturate. The transimpedance versus hole concentration for a fixed electron concentration,  $n \approx 5 \times 10^{10} \text{ cm}^{-2}$ , is depicted in Fig. 2(b). For the higher hole densities,  $R_T \propto p^{-\beta}$  with  $\beta$  varying between 1.2 at the lower temperatures and 0.8 for the higher ones. The transimpedance seems again to saturate at low densities. Note that for  $n, p < 1.6 \times 10^{11} \text{ cm}^{-2}$ , the separation between layers is smaller than the mean distance between carriers within a layer. The transimpedance is found to be linear in the temperature for the higher densities as is evident from Fig. 3. At the lower densities we find a much weaker temperature dependence. Experimentally we thus find that for a wide range of parameters, the role of electrons and holes is different and the transimpedance approximately scales according to  $R_T \propto T/pn^2$ . Such a scaling was used to correct the data presented in Fig. 2 for small variations ( $\leq 15\%$ ) in one carrier concentration as the other one is scanned.

At temperatures below 9 K we observe a transition into an insulating phase as the electron density is reduced below  $\approx 5 \times 10^{10} \text{ cm}^{-2}$ . In part, this transition results from the contacts and in part occurs in the sample itself. For  $T < 9 \text{ K}$  the transimpedance no longer satisfies the Onsager relation indicating that transport is no longer

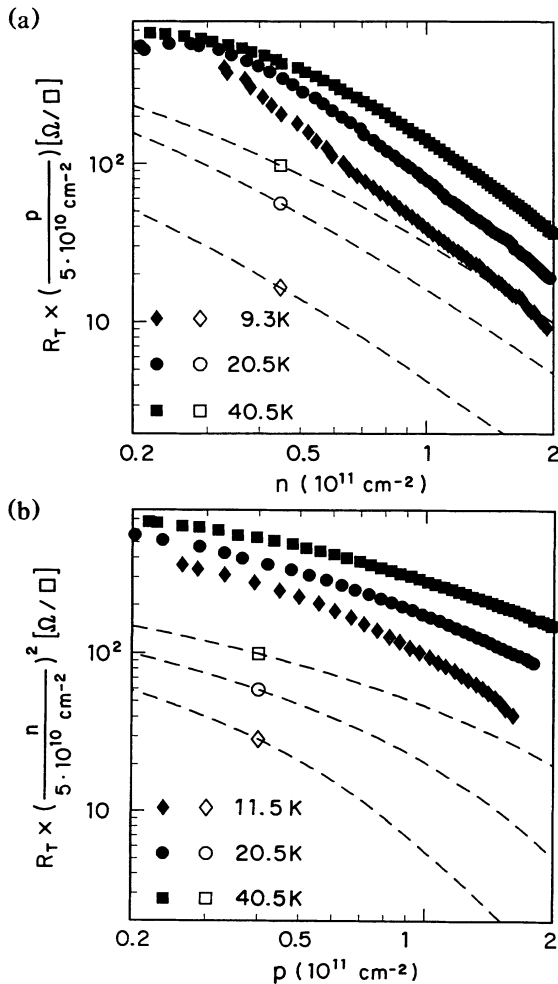


FIG. 2. (a) Corrected transimpedance per square vs electron concentration for three temperatures,  $p \approx 5 \times 10^{10} \text{ cm}^{-2}$ . Solid and open symbols correspond to experimental and theoretical results, respectively. (b) Corrected transimpedance per square vs hole concentration,  $n \approx 5 \times 10^{10} \text{ cm}^{-2}$ .

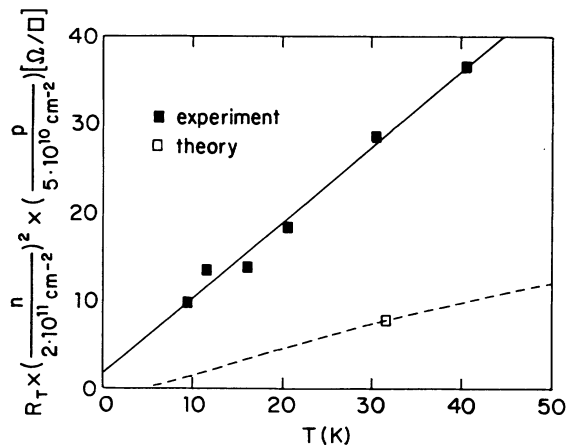


FIG. 3.  $R_T [n/(2 \times 10^{11} \text{ cm}^{-2})]^2 p / (5 \times 10^{10} \text{ cm}^{-2})$  vs temperature for  $p \approx 5 \times 10^{10} \text{ cm}^{-2}$  and  $n \approx 2 \times 10^{11} \text{ cm}^{-2}$ . Solid and open symbols correspond to experimental and theoretical results, respectively (dashed line is for  $p = 5 \times 10^{10} \text{ cm}^{-2}$  and  $n = 2 \times 10^{11} \text{ cm}^{-2}$ ). The solid line is a best fit to the experimental data.

linear. In further discussion we confine ourselves to higher temperatures where the contacts are reliable and transport is perfectly linear.

A number of stray effects [10] might in principle result in an "induced" voltage, the most important of which is a direct carrier transfer between layers by tunneling or leakage. Our sample lends itself to separate measurement of electron and hole leakage currents, both of which were negligibly small. Moreover, a simple ac circuit analysis [10] shows that upon moving the grounding point from *A* to *B*, the ac leakage current polarity is reversed relative to the source. Such an effect is observed only for much higher  $V_B$  when leakage becomes appreciable. Another possibility is a capacitive coupling between lay-

ers. Our results, however, are frequency independent and the measured signal is in phase with the applied one. Finally, rectification of some ac noise or modulation of a dc stray bias by the device acting as a standard field-effect transistor near cutoff is in principle possible. Yet, unlike the measured effect, such a mechanism persists when the driving current is shut off [10].

A natural candidate for an interlayer momentum-transfer mechanism is Coulomb scattering which was first suggested by Pogrebinskii [12] and was found to account for momentum transfer between two parallel 2DEGs [10,11,13], at least when the temperature was not too low. The transimpedance is calculated by Fermi's "golden rule" [13],

$$R_T = \frac{\pi \hbar}{2Te^{2np}} \sum_{k, \sigma_e} \sum_{K, \sigma_h} \sum_q q_x^2 |M(q)|^2 (1 - F_K) F_{K+q} (1 - f_k) f_{k-q} \delta(E_k + E_K - E_{k-q} - E_{K+q}), \quad (1)$$

where *k* (*K*) is the electron (hole) wave vector,  $\sigma_e$  ( $\sigma_h$ ) is the electron (hole) spin, *f* (*F*) is the electron (hole) Fermi distribution, and *q* is the exchanged wave vector. The interaction matrix element *M* is calculated in the random-phase approximation (RPA) [13], assuming zero thickness of the gases,

$$M = \frac{2\pi e^2 \exp(-qa)}{\kappa q D(q, \omega)}, \quad (2)$$

$$D = \left(1 - \frac{2\pi e^2}{\kappa q} \Pi_e\right) \left(1 - \frac{2\pi e^2}{\kappa q} \Pi_h\right) - \exp(-2qa) \left(\frac{2\pi e^2}{\kappa q}\right)^2 \Pi_e \Pi_h.$$

Here  $\kappa$  is the dielectric constant,  $\hbar\omega$  is the energy exchanged in the scattering process, *a* is the separation between the 2D gases, and  $\Pi_e$  ( $\Pi_h$ ) is the electron (hole) polarizability given by Stern [14] and Maldague [15] for zero and finite temperatures, respectively. The sums over electron and hole momenta and spin orientation in Eq. (1) are carried out using the fluctuation-dissipation theorem [16], and after integration over the angle of *q*

$$R_T = \frac{\hbar}{32\pi^2 T e^{2np}} \int_0^\infty q dq \int_{-\infty}^\infty d(\hbar\omega) q^2 |M(q, \omega)|^2 \times \frac{\text{Im}(\Pi_e) \text{Im}(\Pi_h)}{\sinh^2(\hbar\omega/2T)}. \quad (3)$$

For the case of *e-e* scattering we reproduce the results given in Refs. [11,13], though it turns out that the analytic approximation converges to the exact numerical calculation only for layer separations which are considerably larger than the parameters used in the experiment. Interestingly enough, we find that for low carrier densities and  $T \gtrsim \hbar^2 k_F / 2ma$  there is a substantial contribution from coupled plasma modes reflected in the vanishing of the real part of the dielectric matrix determinant *D*. This contribution is neglected in Refs. [11,13]. For the case of

*e-h* scattering, the results depend to some extent on the unknown hole mass. Holelike plasma modes play an even larger role compared with the *e-e* case and under certain conditions dominate the interlayer momentum scattering. Theoretical results for the parameters used in the experiment, and assuming  $M = 6.7m$ , are shown in Figs. 2 and 3 using open symbols. Both the experimental and the theoretical  $R_T$  depend asymmetrically on *p* and *n* due to the different masses. The heavier hole mass leads to a shorter screening length for holes, a lower plasma frequency, and a lower degeneracy temperature. The experimentally measured drag is a factor of 5 to an order of magnitude larger than the calculated one. For  $T = 40.5$  K the calculated and measured transimpedances depend in a similar way on both *p* and *n* while at low temperatures, significant differences develop. The experimental dependence upon *p* becomes weaker than the theoretical one while the opposite is true for the dependence upon electron concentration. The increased discrepancy for lower temperatures is also evident from Fig. 3. This fact, in conjunction with the qualitative similarity at high temperatures, suggests that an additional coupling mechanism might be operative at low temperatures. A possible candidate is an *e-h* binding. Although the binding energy in the presence of free carriers is reduced in the static limit by a factor of  $(2\pi e^2/\kappa)^2 \Pi_e \Pi_h a^2 \gg 1$  compared with the unscreened case, and is therefore smaller than both temperature and kinetic energy, it might be very much enhanced near plasma frequencies where the real part of the dielectric determinant vanishes. The gross quantitative disagreement calls, however, for serious modifications of the simple theory.

Some enhancement of the interaction might result from the disorder [17] present in our system. However, the role of disorder must be limited at the higher electron densities where the electron inverse mean free path is much smaller than a typical wave vector,  $q \approx a^{-1}$ , ex-

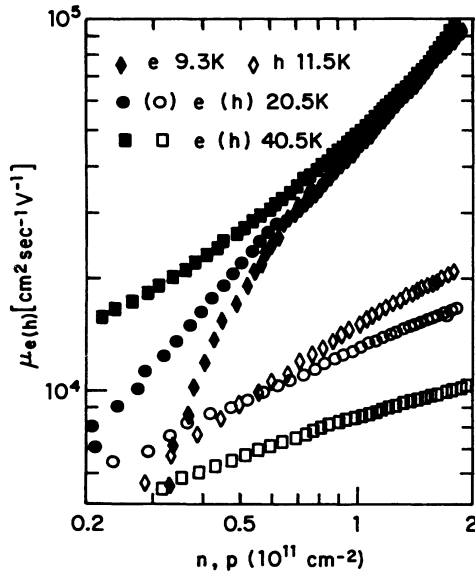


FIG. 4. Electron and hole mobilities vs carrier concentration for three temperatures and the same conditions as in Fig. 2.

changed in the scattering process. Both mobilities versus carrier concentrations are presented in Fig. 4. The mobility of a given layer is practically independent of carrier concentration in the other layer, except for low densities where interlayer screening apparently plays a role. Another possibility is that corrections beyond RPA dominate the scattering. Such a calculation goes beyond the scope of the present Letter and also calls for further theoretical work. We conclude by mentioning that another candidate, namely, acoustic-phonon-mediated momentum transfer, is at least 2 orders of magnitude too small to account for the experimental data.

In summary, we have realized a novel electronic system where two parallel gases of electrons and holes coexist in a proximity allowing for strong interlayer Coulomb interaction. Transport measurements reveal a mutual drag which is a factor of 5 to an order of magnitude larger than expected. The discrepancy is especially large at low temperatures where  $e$ - $h$  binding is more likely to occur.

We are grateful to A. B. Fowler for introducing us to this problem, B. Laikhtman for supplying us with his detailed calculations of the  $e$ - $e$  drag, and A. H. MacDonald

for emphasizing the possible role of disorder. This research was partially supported by the Office of Naval Research.

<sup>(a)</sup>Permanent address: Solid State Institute, Technion-Israel Institute of Technology, Haifa 32000, Israel.

<sup>(b)</sup>Permanent address: Submicron Center, The Weizmann Institute of Science, Rehovot 76100, Israel.

- [1] S. I. Shevchenko, *Fiz. Nizk. Temp.* **2**, 505 (1976) [*Sov. J. Low Temp. Phys.* **2**, 251 (1976)].
- [2] Yu. E. Lozovik and V. I. Yudson, *Pis'ma Zh. Eksp. Teor. Fiz.* **22**, 556 (1975) [*JETP Lett.* **22**, 274 (1975)]; *Solid State Commun.* **19**, 391 (1976); *Zh. Eksp. Teor. Fiz.* **71**, 738 (1976) [*Sov. Phys. JETP* **44**, 389 (1976)].
- [3] Y. Kuramoto and C. Horie, *Solid State Commun.* **25**, 713 (1978).
- [4] I. V. Lerner and Yu. E. Lozovik, *Solid State Commun.* **23**, 205 (1977); *J. Phys. C* **12**, L501 (1979).
- [5] I. V. Lerner, Yu. E. Lozovik, and D. R. Musin, *J. Phys. C* **14**, L311 (1981).
- [6] D. Yoshioka and A. H. MacDonald, *J. Phys. Soc. Jpn.* **59**, 4211 (1990).
- [7] P. Hawrylak and J. J. Quinn, *Appl. Phys. Lett.* **49**, 280 (1986).
- [8] T. Fukuzawa, E. E. Mendez, and J. M. Hong, *Phys. Rev. Lett.* **64**, 3066 (1990).
- [9] J. A. Kash, M. Zachau, E. Mendez, J. M. Hong, and T. Fukuzawa, *Phys. Rev. Lett.* **66**, 2247 (1991).
- [10] P. M. Solomon, P. J. Price, D. J. Frank, and D. C. La Tulipe, *Phys. Rev. Lett.* **63**, 2508 (1989); B. Laikhtman and P. M. Solomon, *Phys. Rev. B* **41**, 9921 (1990).
- [11] T. J. Gramila, J. P. Eisenstein, A. H. MacDonald, L. N. Pfeiffer, and K. W. West, *Phys. Rev. Lett.* **66**, 1216 (1991).
- [12] M. B. Pogrebinskii, *Fiz. Tekh. Poluprovodn.* **11**, 637 (1977) [*Sov. Phys. Semicond.* **11**, 372 (1977)].
- [13] P. M. Solomon and B. Laikhtman, in *Proceedings of the Fifth International Conference on the Physics of Electro-Optic Microstructures*, Heraklion, Crete, 1990 [*J. Superlat. Microstruct.* (to be published)].
- [14] F. Stern, *Phys. Rev. Lett.* **18**, 546 (1967).
- [15] P. F. Maldague, *Surf. Sci.* **73**, 296 (1978).
- [16] G. F. Giuliani and J. J. Quinn, *Phys. Rev. B* **26**, 4421 (1982).
- [17] A. H. MacDonald and B. Altshuler (private communication).

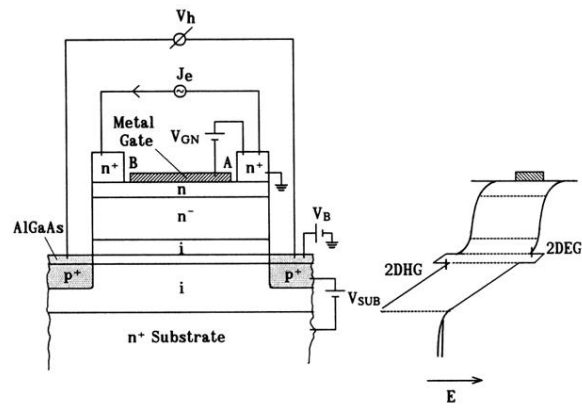


FIG. 1. The structure and schematics of the measurement circuit. On the right-hand side, the band diagram under typical bias is shown.